Journal of
Ceramic Science
and Technology

J. Ceram. Sci. Tech., **06** [01] 31-40 (2015)
DOI: 10.4416/JCST2014-00024
available online at: http://www.ceramic-science.com

Fine Grinding of Bioceramics for Knee Implants with Elastically Bonded Abrasives: Process Modeling and Validation

A. Müller*, B. Denkena

Institute of Production Engineering and Machine Tools, Leibniz Universität Hannover,
An der Universität 2, D-30823 Garbsen, Germany

received June 27, 2014; received in revised form August 1, 2014; accepted September 23, 2014

Abstract

In recent years, there has been steady growth in the application of complex-shaped joint replacement implants and wear-resistant ceramics as implant material. The challenge of implant production remains finishing to an average surface roughness of 20 nm. Tools with elastically bonded diamonds combine grinding and loose abrasive polishing to achieve a high finish with low material removal and thus high shape accuracy – a so-called fine grinding process. This work addresses the working principle of elastic diamond tools in the fine grinding process and the influence of process parameters on the roughness of bioceramics for knee implants. A physical-empirical roughness model based on the number of cutting grains and grain forces was developed and verified as part of the study. The results confirm the hypothesis that the increase of the single-grain force results in the reduction of the surface peaks while taking into account the bond characteristics. For automated use as machine tools for the finishing of all-ceramic implants, continuous wear detection and compensation, by e.g. force controlled polishing, and the temperature stability of the bonds have to be developed.

Keywords: Biomedical ceramics, processing by polishing and fine grinding, elastic tool, surface topography, knee implant

I. Introduction

Manufacturing costs increase exponentially with both target surface quality and workpiece complexity. Up to 50 % of manufacturing costs of ceramic products are attributed to the finishing processes such as grinding and polishing [1,2]. Therefore, new finishing processes are required for the growing share of complex-shaped ceramic components in the optical technology, mould and die production and medical technology sectors. For multiple curved surfaces used in these products, the currently existing finishing processes are very costly. In the area of medical technology, the need for a new finishing technique is even greater owing to the replacement of conventional implant materials such as cobalt-chromium or titanium alloys by advanced high-strength bioceramics like zirconia-toughened alumina.

To reduce wear of joint implants, one possibility is the replacement of metal components by hard, wear-resistant bioceramics used in hip implants. The shape of the articulating surfaces of a hip implant roughly corresponds to a ball joint. Such implants are manufactured in up to 60 individual steps [3]. The manufacturing of the geometry of a knee joint implant with free-form surfaces is more difficult. This would lead to high rates of rejected parts and uneconomical manufacturing chains [4]. Furthermore, there are no uniform standards for the requirements of surface and shape quality of ceramic knee implants. The current target values are based on experiences with ceramic hip prostheses.

* Corresponding author: mueller@ifw.uni-hannover.de

International standards for design and manufacturing of implants describe and specify the tests for ceramics in different applications. They classify and dimension the knee prostheses made of different materials, but the given information is not sufficient for characterizing knee implants. In the literature, surface quality is primarily quantified using the 2D average roughness parameter, *Ra* [5,6]. The Ra is an arithmetic average value of the absolute values of a measured profile. A comparison of common implants by means of three-dimensional measuring technologies shows significant differences in roughness peak height Sp (by multiple 2D measurements averaged *Rp*) and the volume parameters of a topology, e.g. the void volume of the valleys *Vvv* divided by the void volume of the core *Vvc*, apart from the typically known parameters *Ra*, arithmetical mean height of a surface *Sa*, the maximum height *Rz*, the maximum height of the surface *Sz*. All parameters are described in the ISO Standard ISO 23178: Geometry Product Specifications (GPS) – Surface texture. Therefore, in this paper results for the peak height *Rp*, averaged by 512 profile sections from 3D measured surfaces (160 µm x 160 µm) are described.

To finish precision-ground all-ceramic knee implants, a polishing process is needed which works according to the requirements of such a ceramic implant. This means the ability to smooth the roughness peaks of free-formed ceramic surfaces without changing the pre-ground macro-geometry of an implant, the avoidance of polishing suspensions, and the use of the tools in one CNC-machine tool leads to the reduction of the manufacturing steps.

In dental applications ceramic free-form surfaces have been machined manually with elastic pin tools for many years. For shape machining, the ceramic component is treated by means of fine-grinding pins with hard resin bonds. In the following finishing steps, resilient tools with grains in polyurethane or silicone bonds are used. As final manufacturing step, lapping with multiple felt polishing steps and loose abrasive elements (suspension or paste) is performed to achieve the typical dental surface. The post-shaping steps are known collectively as 'polishing' [7].

However, polishing is not conceptually and technologically standardized in DIN 8589 (manufacturing processes) as a manufacturing technology. Depending on the application required, different processes have been established [8–14]. Regardless, high surface qualities are always required after the polishing step, preferably in the nanometer range. In the outdated DIN 4766-T2 (processes for roughness of surfaces; achievable arithmetic average roughness Ra), surface roughnesses of $Ra = 12 - 400\,nm$ are realized by polishing. ISO 1302 (geometric product specifications (GPS) – Indication of surface texture in technical documentation) defines surfaces of $Ra = 7.5 - 60\,nm$ by polishing, lapping or superfinishing [15].

An appropriate classification of the application-specific polishing processes is sub-divisioning in accordance with the principle of material removal and chipping, such as those described by Gessenharter [16]:

(i) physical-mechanical processes;
(ii) physical, but not mechanical, processes;
(iii) chemical removal processes.

Resiliently or elastically bonded grains [7, 10, 16–19] are allocated to category (i). In polishing with elastic-bonded grains, material removal is achieved by means of an abrasive procedure where, typically, the hard abrasive penetrates the softer workpiece surface. This resembles fine grinding processes. Here, physical-mechanical polishing is defined by the type of grain integration:

(i) **Polishing with loose abrasive:** Grains are located between the workpiece surface and the polishing tool. Therefore, grains mainly roll in between the surfaces, generating 3-body-abrasion. This mechanism is called micro-cracking [21]. Examples: CMP, lapping.
(ii) **Polishing with rigidly bonded abrasive:** A ductile removal is achieved by a scratching grain corresponding to grinding wheels. This is called 2-body abrasion and results in a micro-cutting mechanism. Examples: precision grinding, honing.
(iii) **Polishing with elastically bonded grain:** Initially, a grain is fixed to the bond; it scratches the surface by micro-cutting (2-body abrasion). Owing to cutting forces higher than the bond retention forces, the grain is pulled off. Then, the grain rolls between the tool and the surface (micro-cracking, chipping, 3-body abrasion). Examples: belt polishing, dental tools.

First results on the mechanisms and the principle process behavior in polishing of ceramic materials with elastically bonded diamond tools were presented by the authors [21, 22, 23]. Previous studies by Ahn [1] in 2002 used for 5-axis polishing of cold working steel a silicone-base body which was adapted to a pneumatically working spindle head. He shows that the change in roughness is proportionally dependent on the polishing pressure and the polishing grain radius and inversely proportional to the hardness of the steel – similar to the results of loose polishing found by Luo [24]. Thereby, the minimally achievable roughness is limited by the indent depth of the grain.

Brinksmeier *et al.* [10] found out that steel can be work-hardened by grinding with elastically bonded tools. He uses polyurethane-bonded corundum tools in plunge grinding. The tool engagement conditions are different to polishing pins used in this paper (Fig. 1), but he measured specific process forces between 5 and 8 N/mm^2 during the finishing step. They describe the tool mechanisms in three steps: Firstly the tool stiffens, secondly the tool engages in the material and thirdly plastic deformation occurs. During polishing and grinding with elastically bonded tools heat is generated and can be used for grind hardening. An increase in the hardness of the bonding increases the compressive stresses in the subsurface of steel. A comparison of the roughness after polishing with these tools is lacking. Compared to the tools used here, he uses very hard elastic bonds measured with a Grindosonic system. Hahmann [18, 25] described that the hardness of the elastic bonding will not considerably influence the roughness, however, the grain's size will. She showed a significant influence of the infeed and whereas the velocity quotient had a minor effect on the roughness.

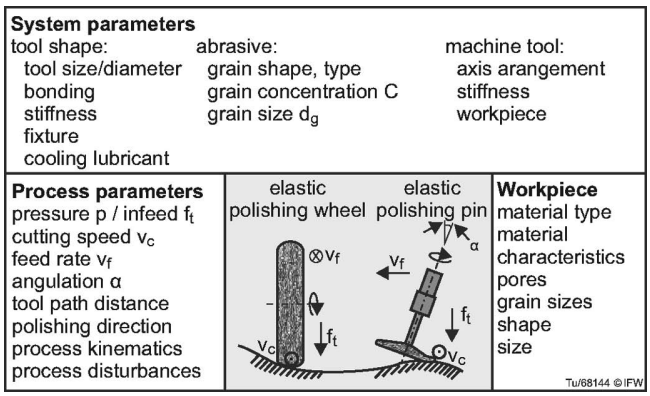

Fig. 1: System and process parameters in resilient polishing.

Latest studies by Sooraj [19] investigated elastomeric bond beads for internal finishing of hardened steel. These "balls" are similar to loose abrasive behavior; thus, the process is described as abrasive flow finishing. He calculates the active number of grains in contact via the bond volume and the grain size. This is comparable with the approach described by the authors in 2009 and 2010 [22, 23]. Within his work, the refinement of the steel surfaces is dependent on the pressure, the grain size, and the elastic properties of the elastic beads, the cutting speed and the calculated number of active grains. In finishing investigations he varies grain sizes, pressure and cuttings speed; and he deduces a regression model for the surface roughness Ra, but a variation of the bond characteristics and a defined variation of the active number of grains are lacking.

The literature review comes to the partially controversial conclusion concerning the effects of the process parameter in polishing depending on the tool used and tool kinematics. Furthermore, important process parameters

are not included in the published results. No further literature on polishing of ceramics with elastically bonded diamond tools exists. A defined process design based on the polishing forces of a single grain and the number of active grains in process is lacking.

Therefore, in the present study the tool performance of elastically bonded polishing tools has been investigated in order to polish biomedical oxide ceramics by the targeted reduction of the roughness peaks. To enable economical and automated polish machining of ceramic implants, it is clear that an increased understanding of the process and key parameters is essential.

II. Material and Methods

(1) Process and system parameters in fine grinding with elastic tools

Elastic tools are available as wheels or pins (Fig. 1). Regardless of the shape and size of the tool, the bond stiffness is influential and can be described by the shore hardness or Young's modulus E [26–28]. The grain types, sizes and concentrations influence the Young's modulus E of the bond. Furthermore, the tool-workpiece contact is influenced predominantly by its use in processing. The pressure is adjustable based on the infeed f_t. The cutting speed v_c, the feed rate v_f, the tool path distance a_p and the angle α mainly influence the time for material removal. Tool path distance and feed rate also determine the polishing time. Beyond this, the surface quality of a ceramic workpiece is highly dependent on the ceramic characteristics: hardness H, fracture toughness K_{ic}, the material combination, and the particle grain size and porosity after the sintering step. At present, there is limited understanding of this comparatively young technology of defined machining with resilient bond [16–20].

(2) Theory

All used parameters and variables described in this paper are listed in the Appendices, Table A1. The majority of the process and system variables of an elastic polishing system can be attributed to two characteristics defined by the authors [1,21,22]: grain number $N_{III,A}$ and grain force F_G. The number of grains $N_{III,A}$ includes all abrasive grains present in a bonding material and is given in 1/mm³. The force F_G defines the part of the process forces acting on one single abrasive grain in normal direction during polishing. The system variables are described by grain concentration C (4.4 ct/cm³ = 0.88 g/cm³ ≙ C100) and grain volume V_g as well as the density of diamond ϱ_g. All together they can be used as grain density γ_o in a bond $\gamma_o = N_{III,A}$. The bond volume connected with the area of contact A_C, the grain distribution and the grain shape are represented by the number of grains in the contact area $N_{II,Ac}$. The process is characterized by cutting speed v_c and feed rate v_f defining the number of grains which slide over the surface during one rotation of the tool. The tool path distance a_p and the surface area to be polished A_p determine the number of grains $N_{II,\,process}$, which slide over this surface in the time interval. The stiffness/hardness of the tool bond, the infeed and the number of grains in contact define the single grain force F_g.

Consequently, our hypothesis is that surface quality is determined by the number of grains sliding over the surface and the force with which the grains are treating the surface. This paper describes the calculation of the characterizing variables and an experimental assessment of this hypothesis.

In a first step, the aim is to describe the active grain number depending on the tool specification (system variables). In the second step, the process parameters are included. Table 1 gives an overview of the calculation procedure.

Table 1: Simulated bond types and their mechanical characteristics.

Step of calculation	Parameter	Symbol	Description
1 System parameters	concentration C grain volume V_g grain density γ_o	$N_{III,A} = \gamma_o$	grain density in the bond material per cm³
	volume of bond V_{bond} contact area A_c height of bond h_p	$N_{II,Ac}$	number of grains in the contact area
	distribution of grains grain shape	$N_{II,A}$	number of grains contacting the surface
	cutting speed v_c feed rate v_f	$N_{II,Ac,vc}$	number of grains sliding over the surface per tool rotation
2 Process parameters	tool path distance a_p size of surface to be polished l_p, w	$N_{process}$	number of grains sliding over surface in the process
	hardness and elasticity of bond H, E numbers of grains $N_{II,Ac}$	F_G	single grain force

(3) Calculating the number of active grains in contact $N_{II,Ac}$

At this point, the conceptual model of cubic unit cells is used to describe the grain distribution in the bond material [29]. The bond material is subdivided into cube elements (CE). Each cube is equivalent to one cubic unit cell. Assuming that the grains and CEs are isotropic, the edge length of the cube is constant and can be calculated. The number of grains in one CE is given by the CE structure (e.g. primitive, hexagonal close packed (HCP), face-centered cubic (FCC) or diamond lattice). The number of grains in the tool bond is constant, thus the grain density γ_o is described equivalently to grinding (Eq. 1) [29].

$$N_{III,A} = \frac{c}{V_g \cdot \rho_g} = \gamma_o \tag{1}$$

Assuming a constant grain density γ_o, the number of grains contacting the surface $N_{II,Ac}$ varies only by the given CE structure (Fig. 2). The number of CEs N_{CE} is calculated by the quotient of the number of grains in the volume $N_{III,A}$ and the number of grains per CE $N_{g,CE}$.

$$N_{CE} = \frac{N_{III,A}}{N_{g,CE}} \tag{2}$$

The number of stacked CE-layers N_{layer} is calculated based on the edge length of the cube element a_c. The height of the overlying bond height is h_p and the cube volume V_{CE} (Eq. 3). The cube volume is calculated based on the surface-contacting bond V_{bond} and the number of CE (Eq. 4).

$$N_{layer} = \frac{h_p}{a_c} = \frac{h_p}{\sqrt[3]{V_{CE}}} \tag{3}$$

$$V_{CE} = \frac{V_{bond}}{N_{CE}} \tag{4}$$

with

$$V_{bond} = A_c \cdot h_p \tag{5}$$

Thus, the number of CEs in the contacting surface $N_{CE,layer}$ is determined by the number of CEs N_{CE} and the number of stacked layers N_{layer}.

$$N_{CE,layer} = \frac{N_{CE}}{N_{layer}} = \frac{A_c}{a_c^2} \tag{6}$$

Depending on the cubic cell structure (number of grain planes in one cubic element $N_{CE,planes}$) and the number of grains in one CE $N_{g,CE}$, a different number of active grains is calculated. Therefore, these grains penetrate the bottom layer of the bond and take an active part in the fine-grinding process.

$$N_{II,A_c} = \frac{N_{CE,layer}}{N_{CE,planes}} \tag{7}$$

$$\frac{N_{II,A_c}}{A_c} = N_{II,A} \tag{8}$$

Assuming a constant grain density (Eq. 1), only system parameters resulting from tool specification influence this number of grains $N_{II,A}$. The average grain size d_g belongs to the diameter of the grain shape (e.g. ball, double taper, double pyramid, double frustum of pyramid) (Fig. 3).

Inserting Eq. 7 in Eq. 8 the numbers of grains per unit of area $N_{II,A}$, where $N_{G,plane}$ is the number of grains in one cube element plane:

$$N_{III,A} = \frac{\gamma_0}{A_c} = \frac{\frac{N_{CE,layer}}{N_{G,plane}}}{A_c} \tag{9}$$

If the Eq. 2 – 6 and 1 are inserted in Eq. 9, the number of grains per unit of area $N_{II,A}$ is calculated by Eq. 10.

$$N_{II,A} = \frac{\gamma_0 \cdot V_{CE}^{1/3} \cdot A_c}{N_{g,CE} \cdot h_p \cdot N_{CE,planes}} = \frac{\gamma_o^{2/3} \cdot A_c^{4/3} \cdot h_p^{-2/3} \cdot N_{g,CE}^{-2/3}}{N_{CE,planes}} \tag{10}$$

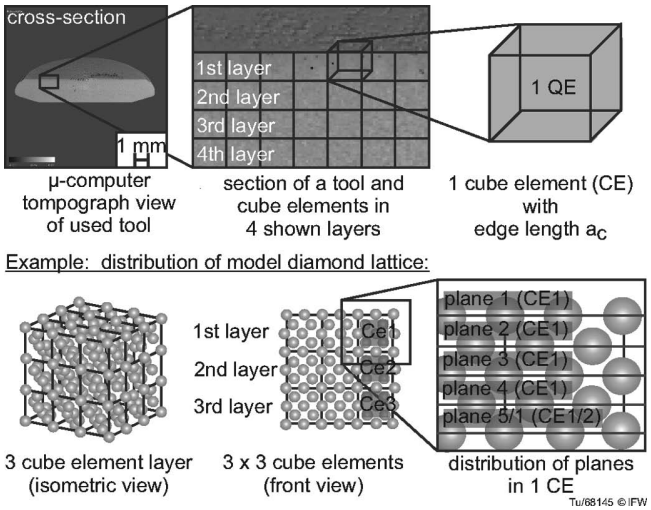

Fig. 2: Grain distribution, definition of cube elements, layers and planes.

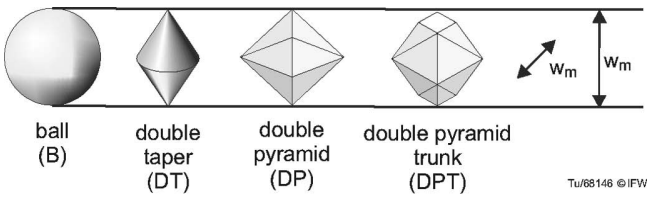

Fig. 3: Grain shapes used in calculation.

Figs. 4 a-c present the results for the number of grains in the surface-contacting bond layer $N_{II,A}$ (Eq. 10) for three different grain sizes d_g, varying bond material (polyurethane and silicone) and diamond grain concentration C. For this calculation a diamond lattice and a ball shape were used. SEM images were made of the bond to count the number of grains. The SEM images were divided in 0.1 x 0.1 mm² areas. Each tool was counted eight times and of each tool type three tools were counted. The standard deviation in counting was 4.8 grains at maximum. The ball shape is the form with the lowest differences to the counted amount of grains.

The highest deviation was found for a polyurethane tool (C115) and a silicone tool (C100) with the grain size d_g = 30 µm – 40 µm (Fig. 4c). This results from the grain size distribution of the diamond powder. According to the manufacturer's instructions of type RVM-N a diamond grain type of 15 µm – 25 µm contains 7.5 % of grains smaller than 15 µm and coincidently only 2 % of grains bigger than

25 µm (Fig. 4b). However, the distribution of PDA type d_g = 30 µm – 40 µm contains only 50 % of grains between 33.5 µm and 36.5 µm.

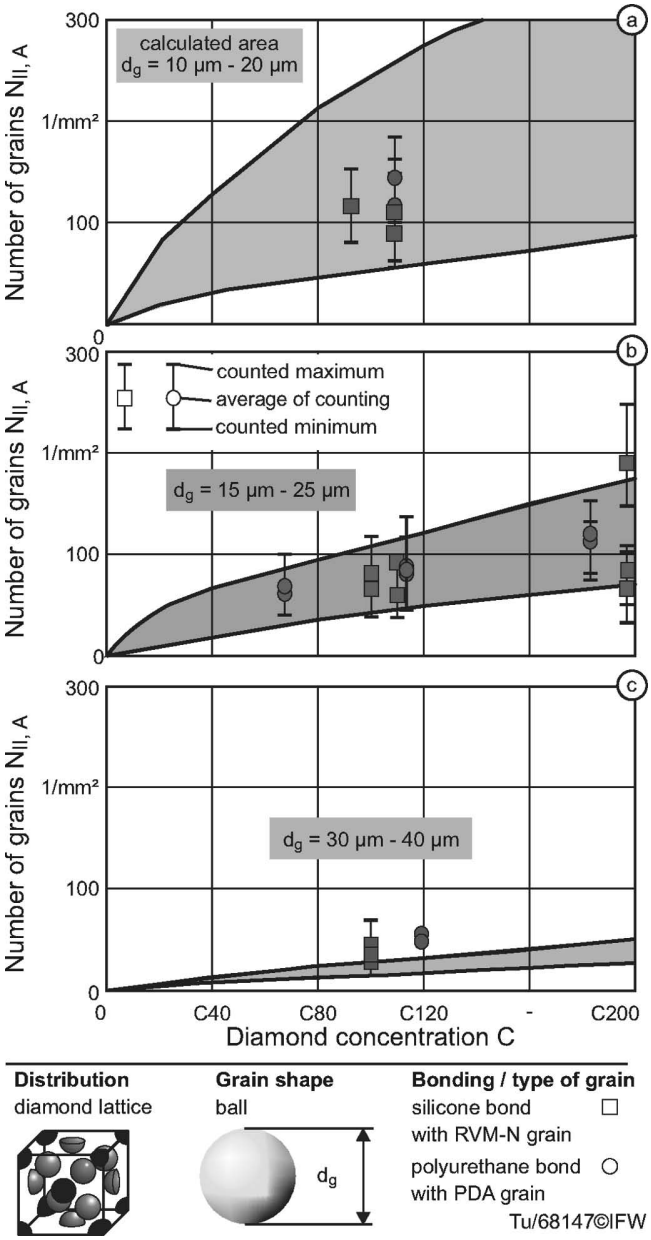

Fig. 4: Counted number of grains $N_{II,A}$ for three different grain sizes.

To establish a link between $N_{II, A}$ and the process parameters tool path distance a_p, feed rate v_f, cutting speed v_c and the size of the surface that has to be machined, the number of active grains in the complete polishing process $N_{process}$ can be calculated by means of two different solutions. On the one hand the number of grains in the contact area per tool rotation $N_{II, A}$ can be multiplied with the number of tool rotations in the complete process $n_{process}$. On the other hand, the process time $t_{process}$ can be multiplied with the amount of grains per time unit $N_{II, Ac, vc}$. Both solutions have the same result.

The number of rotations $n_{process}$ is defined by the process time $t_{process}$ and the time needed for one tool rotation t_r. The process time in contact is calculated from the time needed for one tool path t_{path} and the number of tool paths n_{paths} on the area that has to be polished. The time t_{path} is determined by the feed rate v_f and the length of one path l_p. The number of paths n_{path} results from the tool path distance a_p and the width w of the area that has to be polished.

$$n_{process} = \frac{t_{process}}{t_r} = \frac{t_{path} \cdot n_{path}}{t_r} = \frac{l_p}{v_f} \cdot \frac{w_p}{a_p} \cdot \frac{1}{t_r} \qquad (11)$$

Thus, the number of grains in the complete polishing process of an area ($l_p \cdot w_p$) is computable with Eq. 12 and the tool diameter d_p.

$$N_{process} = n_{process} \cdot N_{II,A_c} = t_{process} \cdot \frac{N_{II,A} \cdot A_c \cdot v_c}{\pi \cdot d_p} \qquad (12)$$

All variables of Eq. 12 are known or can be determined with simple methods. Therefore, a calculation of the active number of grains in process is possible.

(4) Determination of polishing force per grain F_G

During fine grinding with elastic polishing tools, the bond is deformed when contacting the workpiece surface. The theoretical model for the contact surface can only be calculated based on the assumption of an ideal deformation of the tool. From a mechanical point of view the deformation of the tool bond can be considered as a bending of a disc [30]. But the theory of disc bending presupposes that the bending is small compared to disc thickness and the deflection is much smaller than the disc thickness to avoid distortion. Both conditions are not met for the application of the elastic polishing pin. Hence, the contact area A_c is computed here with help of finite element methods. For determining the contact area and contact forces of the bond with the surface for different tool bond types (Table 2) as well as different infeeds f_t, Ansys 14.5 was used.

The bond can be interpreted as an elastomer, which is simulated as linear-elastic material. Since the tool is not loaded until failure, hyperelasticity can be neglected. The shank is firmly connected to the bond. On the shank of the tool a shift f_t is applied. The friction coefficient µ is 0.5 and the Poisson ratio ν is 0.477. The simulated contact area A_c and the acting normal force are as an example shown for silicone bond in Figs. 5 and 6.

The contact force F_N increases with the Young's modulus E and with infeed f_t. The inclination angle α shows a lesser influence. F_N can be described by a quadratic regression model. The correlation coefficient for F_N is given in Table 3. Parameters are significant for $p < 0.1$ (student distribution, confidence interval 99 %, t-value = |2.423| for significance for 40 degrees of freedom). F_N can be calculated in Eq. 13 with the coefficient of determination of 0.99.

$$F_N = b \cdot E + c \cdot f_t \cdot \alpha + d \cdot f_t^2 + e \cdot E \cdot f_t \qquad (13)$$

With regression coefficient b = -0.002; c = -0.236, d = 0.208 and e = 0.054. Fig. 7 shows the results of the regression model in accordance with measured and computed forces. Forces were measured in process with a rotational force dynamometer Kistler HS-RCD 9125 A. Eq. 13 allows calculation of the contact force without additional numerical methods. Dividing F_N by the active number of grains in contact $N_{II, Ac}$, the single-grain force F_G is computable.

Table 2: Simulated bond types and their mechanical characteristics.

Type of bond	Grain concentration C	Grain size d_g in µm	Shore A hardness of bonds	Young's modulus E in N/mm²
silicone	50	20	78.0	11.07
silicone	100	20	81.0	13.27
silicone	200	20	95.0	58.40
polyurethane	100	20	90.3	28.56

Table 3: Correlation coefficient matrix for F_N.

	E	$f_t \cdot \alpha$	f_t^2	$E \cdot f_t$
E	1.000	-0.347	0.439	-0.743
$f_t \cdot \alpha$		1.000	-0.767	0.001
f_t^2			1.000	-0.446
$E \cdot f_t$				1.000

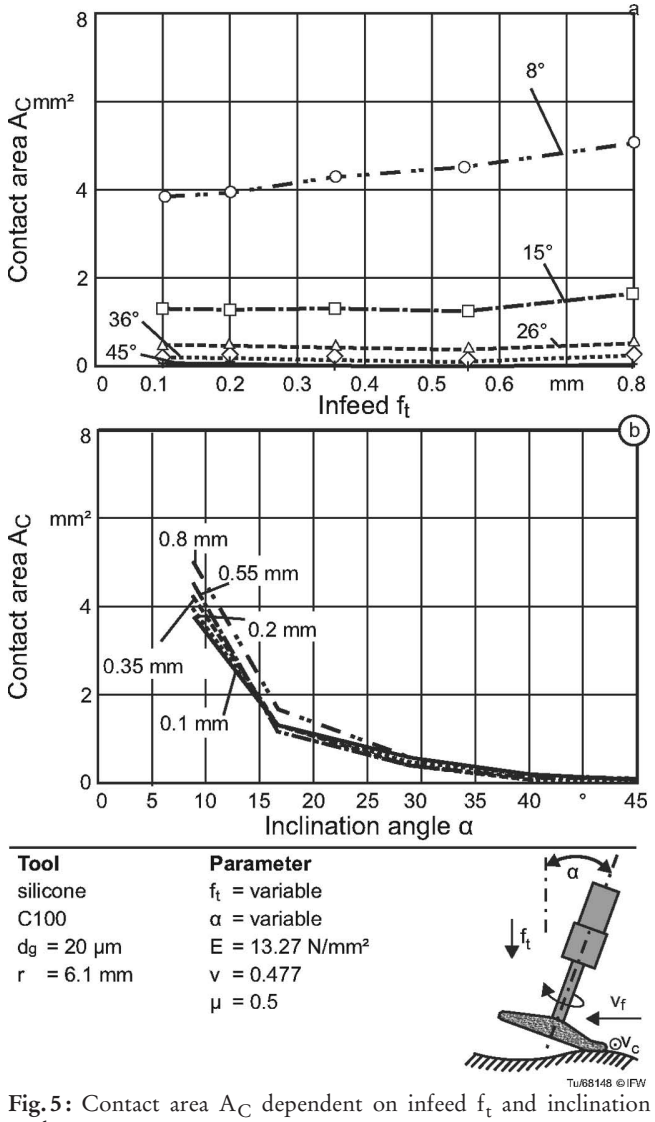

Fig. 5: Contact area A_C dependent on infeed f_t and inclination angle α.

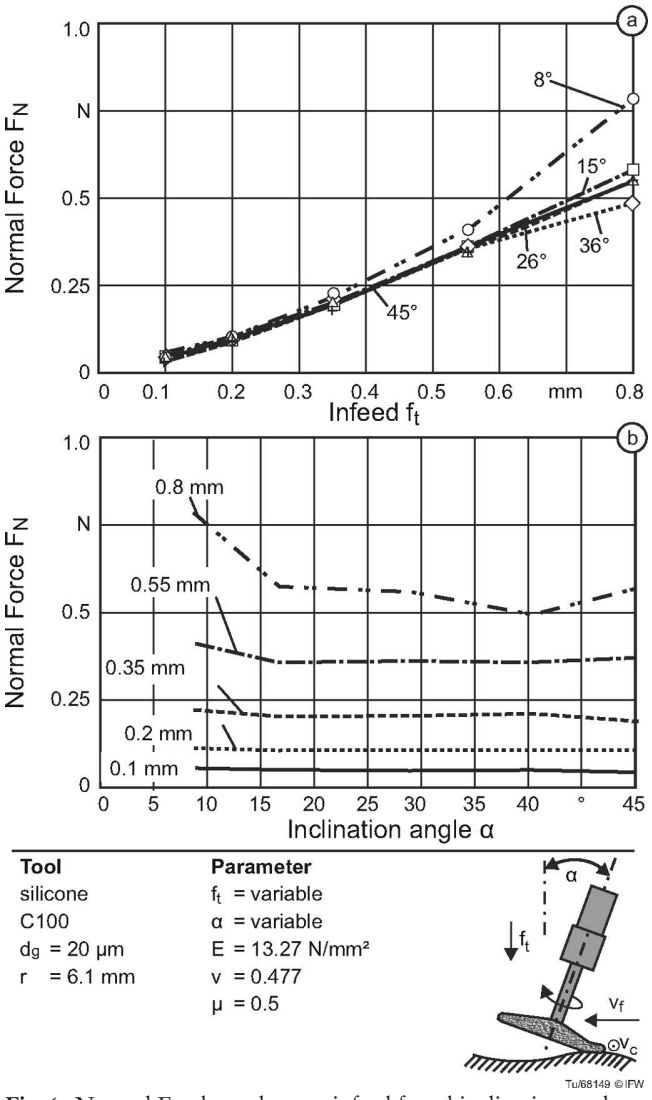

Fig. 6: Normal F_N dependent on infeed f_t and inclination angle α.

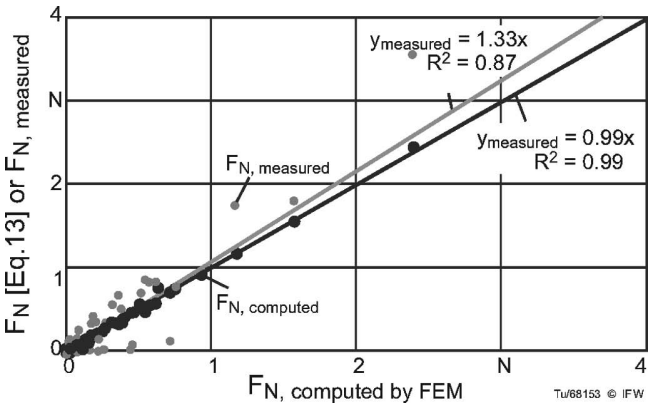

Fig. 7: Comparison of predicted normal force F_N [Eq.13], measured forces and computed forces.

III. Machine Tools, Workpieces and Measurement Equipment

Fine-grinding experiments were done with elastic polishing pins (Fig. 1) on a 5-axis machine tool (Röders RFM 600 DS). In the machine tool, a laser length measuring system is integrated. No cooling lubricant was used. The investigations were conducted on sintered, HIP-ed and pre-ground biomedical alumina oxide ceramic workpieces with an average grain size of 1.75 µm, a density of 3.97 g/cm^3, a hardness of 2040 HV1, a Young's modulus E of 407 GPa and a fracture toughness K_{Ic} of 3.2 MPa m$^{-1/2}$.

The process parameters cutting speed v_c, feed rate v_f and tool path distance a_p, the infeed f_t and the inclination angle α were varied in five steps in a central composite design of experiments. Repetitions were done twice for the central point, which are shown as a range in the result graphs. The bond type, the grain size and the grain concentration were varied at the central point, too.

Roughness was measured with an optical white light microscope (Nanofocus, µSurf). The lens has a magnification of 100. Thus, a measuring field of 160 x 160 µm^2 was possible. The vertical measuring range is 0.08 mm with a vertical resolution of 1.5 nm. In the investigations the average roughness value Sa was determined based on EUR 15178 N. Rp was calculated based on DIN EN ISO 4287 as an average value of 512 profile sections. A Gaussian filter of 0.08 mm was used. ΔRp means the shift of initial roughness to roughness after polishing $\Delta Rp = Rp_0 - Rp_1$. ΔRp is used owing to the fact that the initial roughness from pre-grinding on different specimen cannot be kept constant.

IV. Results

Owing to that fact that the number of grains $N_{process}$ and the single grain force F_G cannot be directly varied as a parameter during polishing, in the investigation the process parameters cutting speed v_c, feed rate v_f, tool path distance a_p, infeed f_t, inclination angle α and the system parameters bond type, grain size d_g and grain concentration C were systematically examined.

In this paper, the results will be split up by the influence of the number of grains $N_{process}$ (See section IV. (1)) and the influence of the force per grain F_G (section IV,(2)) on the refinement of the roughness (peak height Rp). The shift of Rp (ΔRp) is always plotted on the Y-axis. The number of grains is influenced by the process parameters cutting velocity v_c, feed rate v_f, tool path distance/overlap a_p and the system parameters grain size d_g and grain concentration C. The force per grain is affected by the infeed f_t, inclination angle α, the number of grains and the Young's modulus E of the bond. Process and system parameters are plotted on the x-axis. On the 2nd axis of diagrams the related number of grains $N_{process}$ or the force per grain F_G is given. More detailed results were described by the authors [31].

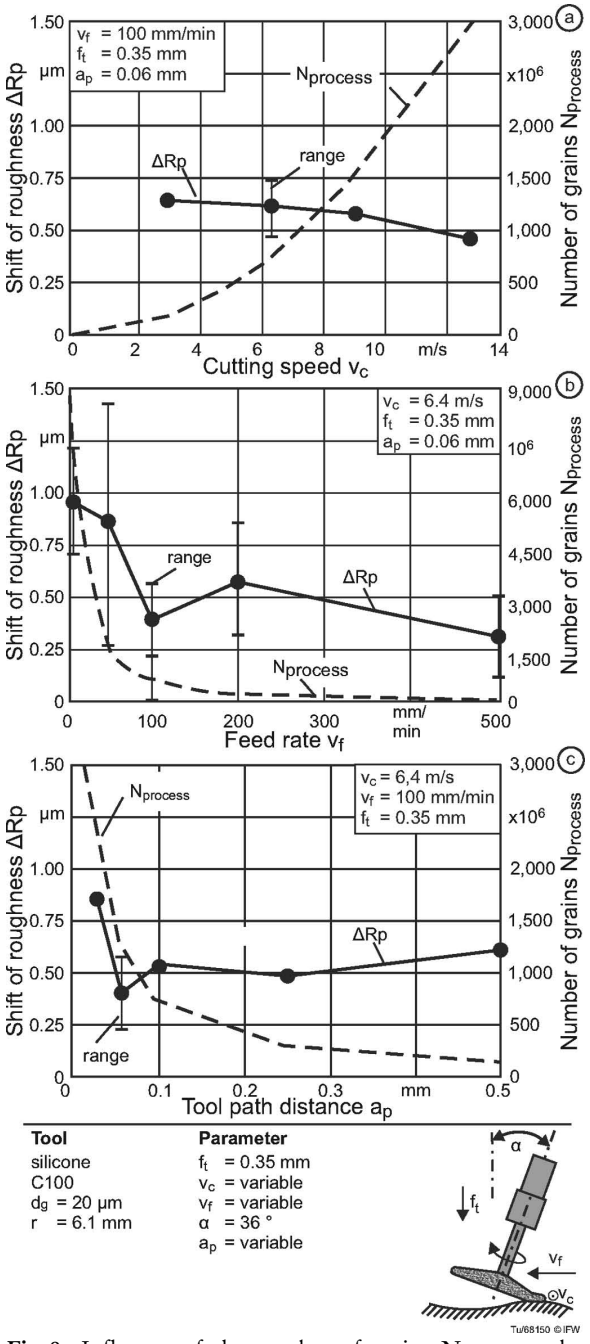

Fig. 8: Influence of the number of grains $N_{process}$ and relating parameter.

(1) Influence of number of grains on roughness

The cutting speed v_c has a considerable influence on the number of active grains (Fig. 8a). However, in case of increasing cutting speed no significant impact could be found. On average a slight decrease could be found for in-

creasing cutting speeds and thus with increasing number of grains. The effect of increasing cutting speeds is overlapped by the tool wear behavior. If the cutting speed is increased, the friction between bond and workpiece surface and therefore, the contact temperature rises. Elastic silicone bonds are not wear-resistant at temperatures over 200 °C. The grains break out owing to a burned bond. In the case of low cutting speed fewer grains are active. So, the normal force F_N is transmitted to the workpiece by a lower number of grains. This increases the force per active grain. If the polishing force exceeds the bond retention forces, the grain will break out of the bond.

The slower the tool moves, the more frequently the grains grab into the material. Thus, if the feed rate is reduced, the roughness peaks are significantly reduced (Fig. 8b). However, decreasing the feed rate means the reduction of the process productivity. In addition, the tool path distance a_p contributes to the productivity of the process. A smaller tool path distance significantly increases the number of active grains. The same behavior is shown for ΔRp (Fig. 8c). In case of $a_p < 0.1$ mm, the tool wear strongly increases.

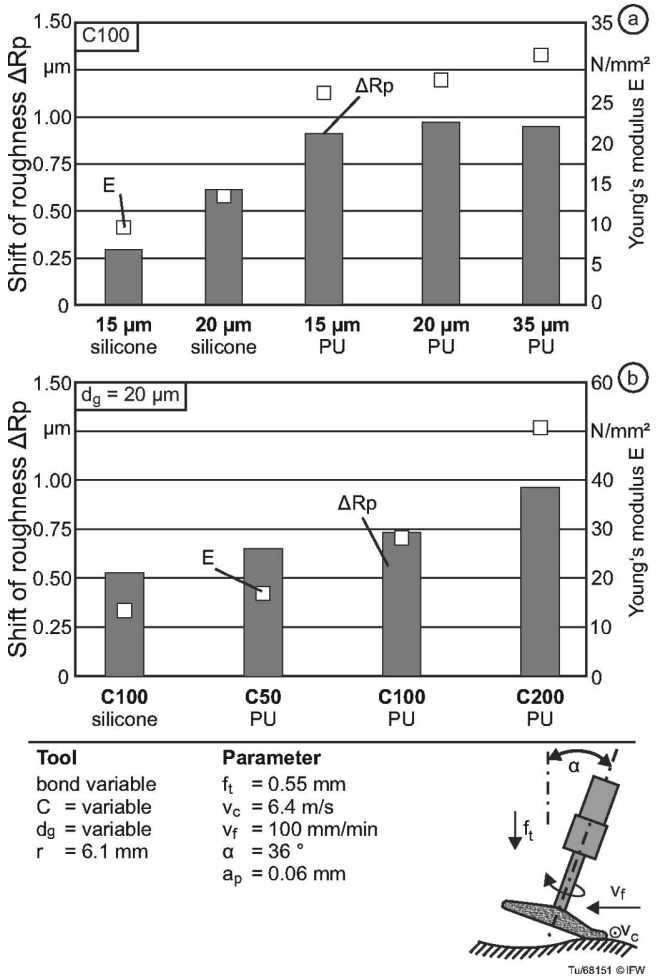

Fig. 9: Influence of grain concentration and grain size.

As described before, the grain size (Fig. 9a) and the diamond grain concentration (Fig. 9b) influence the number of grains in the bond. The tendency that the roughness is influenced more with increasing grain size d_g can be confirmed for both types of bond. In case of constant concentration, the grain size also affects the number of grains due to a constant diamond weight in the bond. If the grain size is constant (Fig. 9b), the roughness changes more if the grain concentration and the Young's modulus rises. This confirms the effect of a higher number of grains. The ability to change the roughness is higher for the tool with polyurethane, which has higher bond stiffness/Young's modulus (Table 1).

(2) Influence of force per grain on roughness

The infeed f_t causes an increase in the axial forces during fine grinding. This was shown in Eq. 13. In Fig. 10 the acting grain force is shown for increasing f_t. If f_t increases from 0.1 mm to 0.8 mm Rp was shifted by 0.9 µm in the same way. If the inclination angle α rises, the acting grain forces rise too, owing to a decreasing contact area of the bond. In this case the roughness decreases, which was shown by the shift of ΔRp by 0.5 µm.

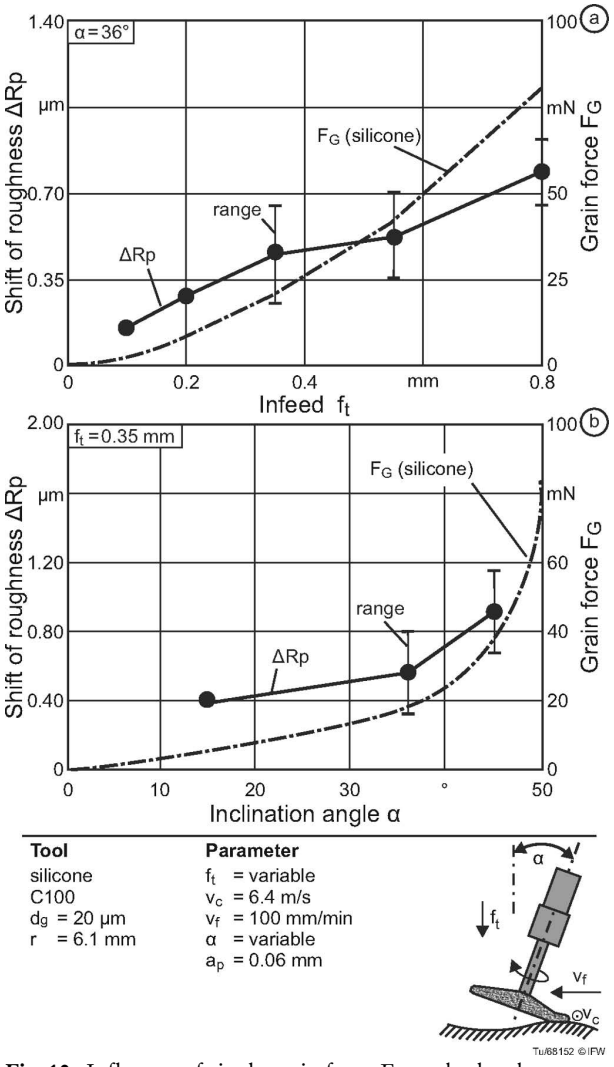

Fig. 10: Influence of single grain force F_G and related parameters.

Concerning the tool behavior under the influence of a variable inclination angle, it was possible to show, that the influence of the grain force on ΔRp is higher than for the active number of grains. For changing the angle from 15° to 45° ΔRp is shifted by 0.5 µm. In this case the active number of grains in process $N_{process}$ falls from $6.32 \cdot 10^9$ to $0.28 \cdot 10^9$ grains. However, the acting single grain force rises from 2.5 mN to 46 mN.

Table A.1: Symbols used in calculation.

Symbol	Meaning	Symbol	Meaning
a_c	Edge length of one CE	$N_{II,\,process}$	Number of active grains in process (in area)
A_c	Contact area	$N_{III,A} = \gamma_o$	Number of grains in bonding volume = grain density
a_p	Tool path distance	N_{layer}	Number of stacked layers in the tool bond height
A_p	Area to be polished	n_{path}	Number of tool paths in area A_p
C	Grain concentration	$N_{process}$	Number of grains in complete process
d_g	Grain size	$n_{process}$	Number of tool rotations in complete process
E	Young's modulus	t_{path}	Time needed for one tool path
F_G	Active grain force	$t_{process}$	Process time
F_N	Normal force	t_r	Time needed for one tool rotation
f_t	Infeed	V_{bond}	Volume of bond
h_p	Height of polishing tool	v_c	Cutting speed
l_p	Length of area A_p	V_{CE}	Volume of one CE
N_{CE}	Number of CEs	V_g	Volume of grains
$N_{CE,\,layer}$	Number of CEs in the contacting surface layer	v_f	Feed rate
$N_{CE,\,planes}$	Number pf planes in one CE	w_p	Width of area A_p
$N_{g,\,CE}$	Number of grains in one CE		
$N_{G,\,plane}$	Number of grains per CE plane	α	Inclination angle
$N_{G,\,plane}$	Number of grains in one CE plane	ν	Poisson's ratio
$N_{II,\,A}$	Number of active grains per area unit	ϱ_g	Density of diamond
$N_{II,\,Ac}$	Number of active grains in the contact area	μ	Friction coefficient

Table A.2: Additional Abbreviations.

Abb.	Meaning	Symbol	Meaning
CE	Cube element	PVA	Grain type of Element Six Ltd.
FCC	Face centered cubic	RVM-N	Grain type of Diamond Innovations, Inc.
HCP	Hexagonal close packed	SEM	Scanning electron microscopy
PU	Polyurethane		

V. Conclusions

The application of ceramics in complex implants, e.g. knee joint implants, exhibits an altered stress situation compared to conventional implants made of steel and polyethylene. Ceramics can withstand these stresses owing to very high compressive strength. However, they break brittle under tensile loads. The mechanical characteristics of an implant are not only determined by design, but by flaws in the microstructure of the ceramic substrate. Chemical properties, different phases, microstructure and surface behaviour affect the prospects for selling an implant. These properties in turn are dependent on the manufacturing process, which is determined by the raw material, the sintering process and the particularly with the finish machining.

To achieve defined surface characteristics a polishing tool was needed to precisely machine free-formed ceramic implants. A polishing process with elastic tools that is able to meet the given requirements on surface finish and shape accuracy has been identified. To use elastic tools in automatic machining, the process know-how must be gained in order to estimate the needed surface finish. This know-how is based on the acting grain force and the number of active grains in process.

The results confirm the hypothesis that the increase of the single grain force results in the reduction of the surface roughness peaks while taking into account the bond characteristics. In case of higher forces, a single grain grabs easily into the material, smoothes the roughness peaks and thus, roughness is refined. As shown in section IV. (1) the number of grains shows a considerable influence on roughness, too. The influence of the cutting speed is not significant owing to an overlap with the bond characteristics. Decreasing feed rate and tool path distance, increasing grain concentration, rising infeed and inclination angle lead to an improvement of the ceramic surface quality.

Now, a transfer of process knowledge from the small elastic polishing pins to larger, in actual machining processes usable tools must be carried out [29]. There is enormous potential for the development of elastic polishing tools. For automated use as machine tools for the finishing of all-ceramic implants the following challenges have to be solved: wear detection and compensation, by e.g. force-controlled polishing, and the temperature stability of the bonds.

Acknowledgements

The investigations described in this paper have been conducted with the support of the German Research Foundation (DFG) within the framework of the collaborative research center CRC 599 "Sustainable Bioresorbable and Permanent Implants of Metallic and Ceramic Materials".

References

1 Ahn, J.H., Lee, M.C., Jeong, H.D., Kim, S.R., Cho, K.K.: Intelligently automated polishing for high quality surface formation of sculptured die, *J. Mat. Proc. Techn.*, **130 – 131**, 339 – 344, (2002).

2 Jain, V.K.: Abrasive-based nano-finishing Techniques: an overview, *Mach. Sci. and Techn.*, **12**, 257 – 294, (2008).

3 Lenk, R.: State of the art in ceramic manufacturing. In: ceramic in orthopaedics – bioceramics and alternative bearings in joint arthroplasty, 10th Biolox Symposium. Washington D.C., USA, June 10 – 11, 175 – 179, 2005.

4 Weiner, M.: Long-life implants, (in German), *Fraunhofer-Magazin*, **3**, 46 – 47, (2007).

5 Niemczewska-Wójcik, M.: The influence of the surface geometric structure on the functionality of implants, *Wear*, **271**, 596 – 603, (2011).

6 Blunt, L., Jiang, X.Q.: Three dimensional measurement of the surface topography of ceramic and metallic orthopaedic joint prostheses, *J. Mat. Sci.: Mater. M.*, **11**, 235 – 246, (2011).

7 Heintze, S.D., Forjanic, M., Rousson, V.: Surface roughness and gloss of dental materials as a function of force and polishing time in vitro, *Dent. Mat.*, **22**, 146 – 165, (2006).

8 Porat, R., Yarnitsky, Y.: Polishing diamond mechanisms, the parameter influence of the polishing rate, society of manufacturing engineers, **MR91 – 192,** 12 – 1 – 12 – 18, (1991).

9 Brecher, C., Tuecks, R., Zunke, R., Wenzel, C.: Development of a force controlled orbital polishing head for free form surface finishing, *Prod. Eng. and Develop.*, **4**, 269 – 277, (2010).

10 Brinksmeier, E.; Heinzel, C.; Bleil, N.: Superfinishing and grind-strengthening with elastic bonding system, *J. Mat. Proc. Techn.*, **209**, 6117 – 6123; (2009).

11 Evans, C.J., Paul, E., Dornfeld, D., Lucca, D.A., Byrne, G., Tricard, M., Klocke, F., Dambon, O., Mullany, B.A.: Material removal mechanisms in lapping and polishing, *CIRP An. of Manuf. Techn.*, **52**, 611 – 634, (2003).

12 Westkämper, E., Hoffmeister, H.-W.: Function-oriented lapping and polishing of ceramic rolling elements through characterization of the workpiece surface, *CIRP An. of Manuf. Techn.*, **45**, 529 – 532, (1996).

13 Brinksmeier, E., Mutlugünes, Y., Klocke, F., Aurich, A.C., Shore, P., Ohmori, H.: Ultra-precision grinding, *CIRP An. of Manuf. Techn.*, **59**, 652 – 671, (2010).

14 Karpuschewski, B., Pieper, H.-J., Welzel, F., Risse, K.: Alternative strategies in finishing cylinder running surfaces, *CIRP An. of Manuf. Techn.*, **61**, 559 – 562, (2012).

15 Smith, G.T.: Industrial metrology. Surfaces and roundness, 1st edition. Springer, Heidelberg, 2002.

16 Gessenharter, A.: Polishing structured mould inserts for optical components (in German), 1st edition. Shaker, Herzogenrath, 2006.

17 Wang, G., Wang, Y.: Research on polishing process of a special polishing machine tool, *Mach. Sci. Techn.*, **13**, 160 – 121, (2009).

18 Hoffmeister, H.-W., Hahmann, W.-C.: Superfinishing of bearing rings using elastic bonded grinding wheels. In: 26th Annual Meeting of the ASPE Proceedings, Denver, Colorado, USA, 2011.

19 Sooraj, V.S., Radhakrishnan, V.: Fine finishing of internal surfaces using elastic abrasives, *J. Mach. Tools and Manuf.*, **78**, 30 – 40, (2014).

20 Zum Gahr, K.-H.: Wear by hard particles, *Trib. Intern.*, **31**, 21 – 31, (1998).

21 Denkena, B., de Leon, L., Turger, A.: Roughness prediction for elastic polishing of complex ceramic workpieces. In: Proceedings of the 10th euspen International Conference, Delft, Netherland, 216 – 219, 2010.

22 Denkena, B., de Leon, L., van der Meer, M., Turger, A.: Flexible polishing with bounded grains for complex ceramic endoprostheses. In: Proceedings of the 24th ASPE Annual Meeting, Monterey, California, USA, 96 – 99, 2009.

23 Denkena, B., Köhler, J., Turger, A.: Modeling the polishing process with resilient diamond tools for manufacturing of complex shaped ceramic implants. In: ASPE Annual Meeting, Denver, Colorado, USA, 2011.

24 Luo, J.: Integrated modeling of chemical planarization for submicron IC fabrication. 1st edition, Springer Berlin Heidelberg, 2004.

25 Hahmann, W.-K.: Innovative approaches for finishing of functional surfaces, in German, 1st edition, Vulkan-Verlag, 2013.

26 Kunz, J., Studer, M.: Determination of the compression-modulus of elasticity based shore A-hardness, (in German), *Kunststoffe*, **6**, 92 – 94, (2006).

27 Sponagel, S., Unger, J., Spies, K.H.: Hardness in connection with cross-linking, strain to rupture and fatigue resistance of an elastomer, (in German), *KGK Kautschuk Gummi Kunststoffe*, **56**, 608 – 612, (2003).

28 Marinescu, I.D., Hitchiner, M., Uhlmann, E., Rowe, W.B., Inasaki, I.: Handbook of machining with grinding wheels, 1st edition, CRC Press by Taylor & Francis Group, LLC, 2007.

29 Kramer, N., Wangenheim, C.: Model based characterization of the grinding wheel effective topography, In: Advances in abrasive technology XI, 11th International Symposium on Advances in Abrasive Technology, Japan, 258 – 263, 2008.

30 Girkmann, K.: Flächentragwerke. Introduction to the elastostatics of disks, plates, bowls and folded plates, (in German), Springer, Wien, New York, 1978.

31 Müller, A.: Polishing ceramic knee implants with flexible diamond tools, (in German), Berichte aus dem IFW, 4/2014, Denkena, B. (Editor), PZH-Verlag, Garbsen, 2014.